Available online at www.sciencedirect.com

SCIENCE DIRECT®

Geoderma 125 (2005) 213–223

GEODERMA

www.elsevier.com/locate/geoderma

Studies of crack dynamics in clay soil II. A physically based model for crack formation

H.-J. Vogel*, H. Hoffmann, A. Leopold, K. Roth

University of Heidelberg, Institute of Environmental Physics, INF 229, 69120 Heidelberg, Germany

Received 11 December 2003; received in revised form 28 June 2004; accepted 20 July 2004
Available online 23 August 2004

Abstract

The temporal dynamics of soil structure is a typical phenomenon exhibited by shrinking clay soil. It causes substantial difficulties for the characterization of soil properties and for the modeling of fundamental processes such as water flow and solute transport. In this paper, we present a model for crack formation that mimics the physical processes involved. The model is based on a lattice of Hookean springs with finite strength and represents linear quasi elastic materials. It reproduces prominent features of the nonlinear dynamics of crack network development observable in nature like the characteristic shape of aggregates and the characteristic angles of bifurcations and also leads to realistic overall appearances of the pattern. The free parameters of the model can be related to physical properties of the material and to the boundary conditions during shrinkage by desiccation and crack formation. We demonstrate the variety of crack patterns through a systematic exploration of the parameters. The different properties of the obtained crack patterns are quantified with respect to a few basic geometric measures that are evaluated for the dynamics of crack formation and for the final crack pattern. The proposed model has the potential to provide the dynamics of material properties which are highly significant for modeling flow and transport in clay soil.

Keywords: Crack pattern; Fractures; Clay soil; Image analysis; Modeling

1. Introduction

The dynamics of crack formation in clay soils presents a major difficulty for modeling the flow of water as well as the transport of dissolved substances and particulate matter. Moreover, the penetration of plant roots and microbial processes are strongly affected by the dynamics of continuous macropores. Clay content, mineralogy and the physical boundary conditions govern the characteristics of a crack network that forms and evolves with decreasing water content. Thereby, a variable network of macropores is

* Corresponding author. Fax: +49 6221 546405.
E-mail address: hjvogel@iup.uni-heidelberg.de (H.-J. Vogel).

0016-7061/$ - see front matter © 2004 Elsevier B.V. All rights reserved.
doi:10.1016/j.geoderma.2004.07.008

formed, which is highly significant for infiltrating water during rainfall events as well as for water evaporation during dry periods. Today, state-of-the-art models of water flow and solute transport are capable of treating water and solute transport within macropores and within the surrounding soil matrix separately to account for the frequently observed preferential flow (e.g. van Genuchten and Wierenga, 1976; Gerke and van Genuchten, 1993; Jarvis, 1994). Assessing preferential flow requires information on the volume fraction of macropores as well as their hydraulic properties, but these are typically not measured explicitly but lumped into effective parameters which have to be fitted to measured breakthrough curves. Hence, the physical meaning of such parameters which are solely related to a certain experiment, remains unclear.

In clay soil, material properties related to macropores as well as the hydraulic properties of the soil matrix are highly variable in time due to the swell–shrink dynamics. The focus of this paper is on modeling the dynamics of the crack network. The final goal is to provide physical parameters as the volume, size, and connectivity of cracks together with the soil bulk density as relevant input for models of flow and transport.

Modeling the dynamics of soil cracks is typically focused on averaged quantities such as the mean crack volume and the average width of cracks as a function of matric potential (Askar and Jin, 2000; Greco, 2002) or as a function of water content and soil depth [Chertkov, 2000]. The detailed geometry of the crack network including the spatial distribution of cracks and their topology is usually neglected. A detailed geometric representation of cracks was presented by Perrier et al. (1995) who applied a fractal fragmentation algorithm to generate crack patterns at hierarchical scales.Horgan and Young 2000 proposed a detailed geometric model for two-dimensional crack patterns in clay soil which produces realistic patterns. However, in both applications, the generating algorithm does not mimic the real physical process of crack formation. Consequently, these models cannot reproduce the dynamics of natural crack patterns.

Physically based models of soil cracking, based on fracture mechanics theory, are still in their infancy and can only consider the propagation of individual cracks (Hallett et al., 1995; Nichols and Grismer, 1997; Hallett and Newson, 2001).On the middle ground between these two extremes, the process of crack pattern formation as a self-organized system was recently explored from the perspectives of statistical physics. They focus on capturing the nature of the fracture process to reproduce the observed characteristic patterns. Typically, the basis of such models is a two-dimensional lattice where the nodes are connected through Hookean springs which break when a critical strain is exceeded (Meakin, 1987; Hornig et al., 1996; Malthe-Sorenssen et al., 1998; Kitsunezaki, 1999). Once a spring is broken, the distribution of stress in the immediate neighborhood is affected and the development of a crack starts reproducing the phenomenology observed in experiments. Alternatively, a network of electrical resistors or fuses can be considered which obeys a similar phenomenology after breakage of single fuses once a critical current is exceeded (Colina et al., 1993).

In this paper we propose a similar model for crack formation in soils which yields the full dynamics of the crack network during desiccation and has the potential to be adapted to natural materials and boundary conditions. We focus on the complex phenomenon of crack pattern development using strong simplifications with respect to the physics of individual crack development. However, it is anticipated that the proposed model can eventually be combined with fracture mechanics theory by calculating the model parameters directly from microscopic properties of the material. In a previous paper (Vogel et al., 2004), a quantitative approach to describe the geometry of two-dimensional crack networks was presented which will be used here to quantitatively compare the simulated crack patterns.

2. The Model

We consider a two-dimensional flat layer where the formation of cracks is due to slow contraction of the material as a result of water evaporation. We assume that the thickness H of the layer is small enough and the characteristic time of evaporation T_e is long enough to avoid gradients in water content within the thin layer, i.e. H^2T_e is much smaller than the diffusivity of water within the thin layer. We also assume that the relaxation of strain caused by

desiccation is the only contribution to the dissipation of energy in the system. Our model to simulate crack formation is similar to those presented by Kitsunezaki (1999), Malthe-Sørenssen et al. (1998) and Hornig et al. (1996). We represent the clay layer by a two-dimensional triangular network of simple Hookean springs. Each node is connected to its six neighbors by a spring with spring constant K and natural length λ, which is the length of the relaxed spring (Fig. 1). Hence, the strain of each individual spring connecting two nodes at the positions $\mathbf{x}_i$ and $\mathbf{x}_j$ respectively is given by

$$\epsilon_{ij} = \frac{|\mathbf{x}_i - \mathbf{x}_j|}{\lambda} - 1, \tag{1}$$

the net force acting on node i through its N_i neighbors is

$$\mathbf{F}_i = -\sum_{j\epsilon N_i} K_{ij} \frac{\mathbf{x}_i - \mathbf{x}_j}{|\mathbf{x}_i - \mathbf{x}_j|} \left[|\mathbf{x}_i - \mathbf{x}_j| - \lambda\right] \tag{2}$$

and the total energy at each node is given by

$$E_i = \frac{1}{2} \sum_{j\epsilon N_i} K_{ij} \left[|\mathbf{x}_i - \mathbf{x}_j| - \lambda\right]^2 \tag{3}$$

We simulate desiccation by reducing the relaxed spring length λ successively starting from $d = |\mathbf{x}_i - \mathbf{x}_j| = 1$ which is the distance of the nodes in the initial lattice in arbitrary units. Reducing λ increases the contracting forces and the total energy within the lattice. If the strain between two nodes exceeds a critical threshold ϵ_{ij}^b the spring will break and hereafter has no more impact on the energy distribution within the network. The breakage of a spring has immediate consequences for the forces on the nodes previously connected by that spring. They are pulled apart by the other springs which are still connected. Hence, the nodes move towards a new location of minimal energy according to Eq. (3). The net force on the nodes can be obtained through Eq. (2) and the new positions $\mathbf{x}'_i$ of the nodes are obtained by solving Eq. (2) for the condition

$$\mathbf{F}_i = 0 \,\forall i. \tag{4}$$

Thereby, the change in position $|\mathbf{x}'_i - \mathbf{x}_i|$ depends on $\mathbf{F}_i$. However, in our model, a node will move only if $\mathbf{F}_i$ exceeds a certain friction μ which is introduced as a static adhesion of the nodes and is one free parameter of the model. This is the major difference compared to the models proposed by Kitsunezaki (1999), Malthe-Sørenssen et al. (1998) and Hornig et al. (1996) where the nodes are connected through additional springs to the ground.

Once a node has moved after the break of a connected spring this movement affects the energy distribution at the adjacent nodes and hence, these nodes may move subsequently. In this way the whole lattice is relaxed towards a new state of minimal energy. This relaxation is allowed to emanate radially

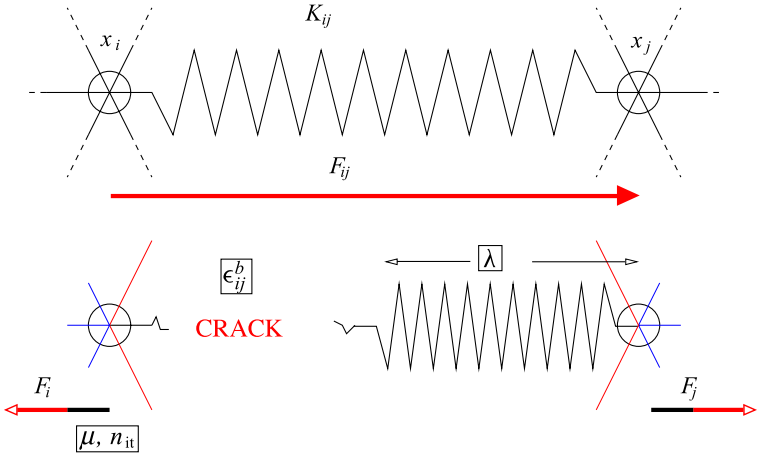

Fig. 1. Schematic sketch of the connection between two nodes at location $\mathbf{x}_i$ and $\mathbf{x}_j$ through a spring with spring constant K_{ij} and natural relaxed length λ. A crack occurs if the strain ϵ_{ij} exceeds the critical strain ϵ_{ij}^b, and the nodes may move apart if the corresponding force exceeds the friction parameter μ. The movement of nodes is calculated for n_{it} iterations (see text).

from the broken location: at each step t of the iteration only those nodes are considered where a connected spring was broken or where the immediate neighbors have moved at step $t-1$. This iterative relaxation of the lattice introduces another parameter which is the maximum number of iterations n_{it}, performed each time after a spring was broken. Depending on the integer value of n_{it} the lattice might not be relaxed completely prior to the breakage of the next spring.

Heterogeneity is introduced through the threshold ϵ_{ij}^{b} of the springs, which is taken for each individual spring from a Gaussian probability distribution with mean $\bar{\epsilon}$ and variance σ^2 and distributed randomly in space. Alternatively, we could choose to vary the spring constants K_{ij} accordingly which would produce the same phenomenology. However the variation of ϵ_{ij}^{b} is computationally more efficient so we chose K_{ij}=1 to be constant. Then, the critical strain ϵ_{ij}^{b} and the friction μ can be expressed as a fraction of the grid constant d=1.

The basic flow chart of the model is given in Fig. 2 together with an example for the location of nodes and the elongation of springs in the initial phase of crack formation. For a given set of parameters, $\bar{\epsilon}$,σ^2,μ and n_{it}, we start with λ=1 meaning the relaxed spring lengths are equal to the distance of the nodes. To break the complete symmetry of the initial lattice, we chose the location of each node not exactly on the coordinates of the triangular grid but added a random value $b\in[-0.1, 0.1]$ to both of its coordinates. In a first step the lattice is relaxed and checked if the strain of some springs exceeds their individual threshold. If yes, the spring which exceeds its threshold most is removed and the lattice relaxed by n_{it} steps. This loop is executed until no more springs have to be removed. Then, the relaxed spring length is reduced by a decrement δ which increases the global energy and the relaxation loop is entered again. The choice of δ is not important as long as the related increment of force is smaller than the friction μ.The simulation ends when $\lambda_{\min}$ as a given minimum value of the relaxed spring length is reached.

Fig. 2 also illustrates the basic phenomenology of the model. After the breakage of a spring at some location in the lattice, the force in the adjacent springs increases (see also Fig. 1). The probability that one of these springs will break next is thus increased considerably. In this way a self-accelerated process is initialized that causes a crack to develop linearly along its tips. This is also a prominent property of natural crack formation.

Due to the heterogeneously distributed thresholds, ϵ_{ij}^{b}, such a self-propagating crack may encounter a more resistant region and may change its direction along the weakest spring. As a consequence, the stress at the resulting bend will increase and the probability of a branching of the crack at this point is increased. An angle of 120° is most likely in terms of total energy dissipation. This reproduces another property of natural crack formation (Vogel et al., 2004). Perpendicular to a crack the springs are relaxed while parallel to a crack the tension is slightly higher compared to the fully connected lattice. Consequently, if a crack tip approaches another already existing crack, a coalescence of the two cracks will be most likely at 90°. This reproduces a third property which is

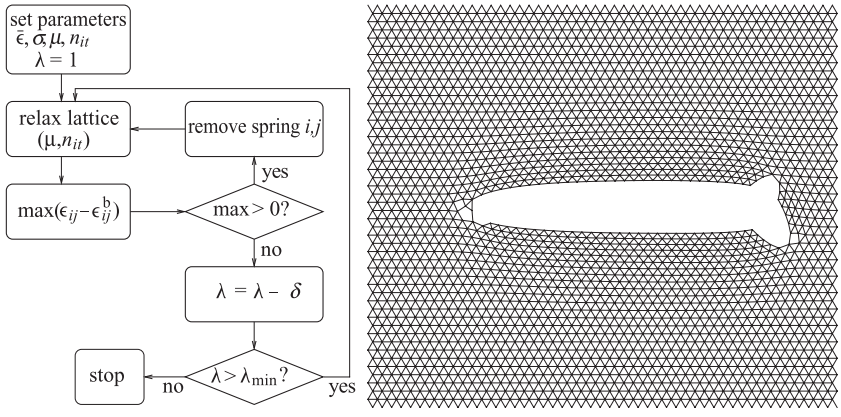

Fig. 2. Flow chart of the model (left) and an example of a lattice after the first springs are broken (see text for more information).

frequently observed for the dynamics of natural crack patterns. Finally, depending on the various model parameters a characteristic network of cracks is formed.

As a first step towards a description of the crack dynamics, we consider a linear elastic material with constant parameters K, $\bar{\epsilon}$ and μ. This model might be linked to classical fracture mechanics through the parameter K which is related to Youngs modulus, the parameter $\bar{\epsilon}$ which is related to the critical stress at failure and μ which is related to interfacial energy. In reality, the situation is more complicated in that the parameters are expected to depend on water content and the crack dynamics is furthermore affected by the compressibility of the medium. However, we believe that our simplified representation capture the essential features of the real system.

As a demonstration of our simple model, Fig. 3 shows an example of a developing crack network together with the energy distribution within the network of springs. The nodes at the boundaries are not allowed to move perpendicular to the boundary. The largest stress is clearly at the tips of growing cracks but also at bends of deflected cracks or in the center of aggregates. Therefore, new cracks are created at these locations.

3. Simulations

The model depends on four parameters: the mean critical strain $\bar{\epsilon}$, its variance σ^2, the friction μ and the relaxation parameter n_{it}. Given all the simplifying assumptions, we interpret these parameters as being related to material properties and physical boundary conditions during desiccation. The mean threshold $\bar{\epsilon}$ is associated with the elasticity of the material and the variance σ^2 describes its microscopic heterogeneity. The friction μ may be inversely proportional to the thickness of the shrinking layer. The relaxation parameter n_{it} may be related to the speed of desiccation. It might be interpreted as a dimensionless quantity relating the characteristic times of external forcing, t_{ext}, to the characteristic times of the internal dynamics t_{int} by $n_{it}=t_{\mathrm{ext}}/t_{\mathrm{int}}$.

In the following we demonstrate the behavior of the model for various settings of the relevant parameters. We keep the mean threshold $\bar{\epsilon}=0.25$ fixed. This is based on the idea that changing $\bar{\epsilon}$ will not enrich the variety of crack patterns, since the same processes act at different values of λ. In Fig. 4 different simulations of the final crack pattern for different values of σ^2, μ and n_{it} are shown.

Obviously, a wide spectrum of crack patterns is obtained. Beside this qualitative conclusion, the different crack patterns can be described quantitatively including their dynamics. This is done using fundamental geometric properties, the Minkowski numbers, as proposed by Vogel et al., 2004. These numbers comprise the area density $A_{\mathrm{A}}=m_0[\mathrm{L}^2\mathrm{L}^{-2}]$, the length density $L_{\mathrm{A}}=m_1[\mathrm{L}\mathrm{L}^{-2}]$ and the number density $N_{\mathrm{A}}=m_2[\mathrm{L}^{-2}]$ of cracks which in the following are referred to as Minkowski densities m_{k} (Mecke, 2000). m_2 is equal to the density of the Euler number which is defined as the number of isolated cracks minus the number of loops in the crack network and herewith describes the connectivity of the crack network. The Minkowski densities of our simulations are expressed in arbitrary units of length which might be related to the pixel size of the images. All Minkowski densities can be obtained as a function of time during crack formation to capture the dynamics of the geometry. In our model time is inversely proportional to the water content which is

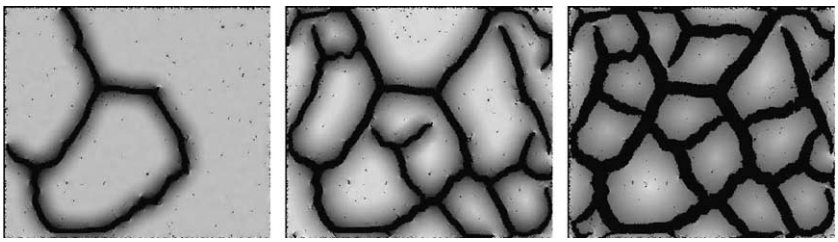

Fig. 3. Different stages of modeled crack formation. The grey values are proportional to the energy of the springs, cracks are black. Brighter grey values represent a higher stress.

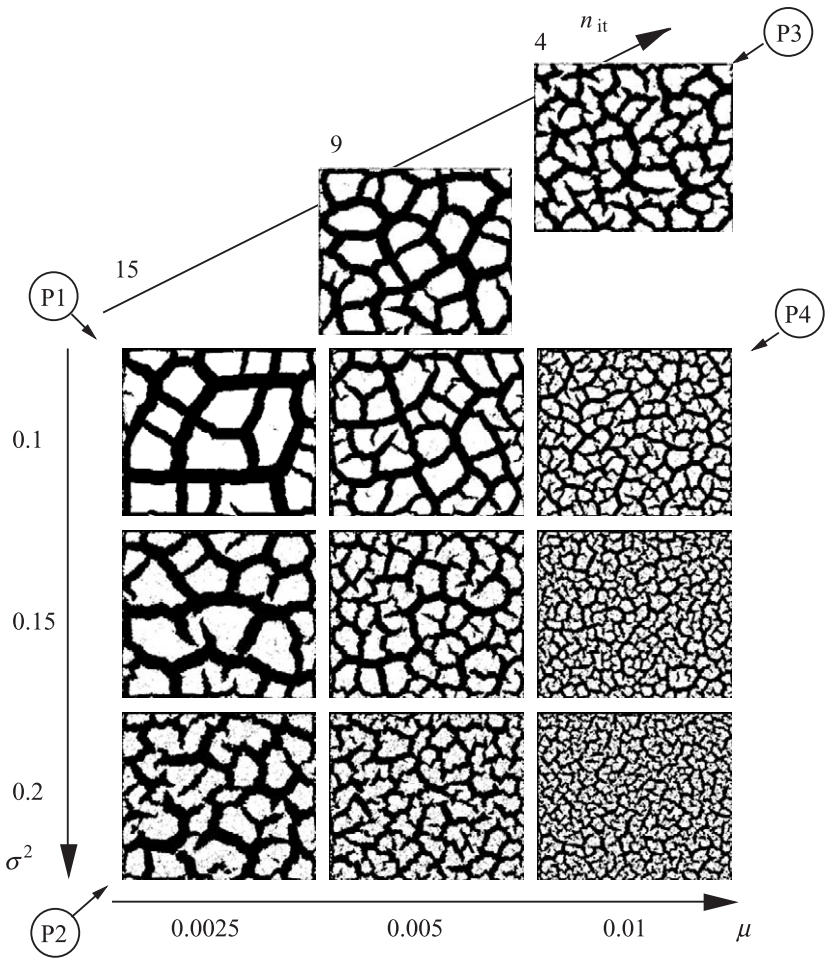

Fig. 4. Crack patterns simulated with various heterogeneity σ^2, various friction μ and various relaxation intensities n_{it}. The series P1→P2, P1→P3, and P1→P4 are subjected to further quantitative analyzes.

directly related to the relaxed spring length λ. Hence, we analyze the geometry of the crack pattern as a function of the mean expansion of the springs $u=1-\lambda$ as a substitute for time or water content, respectively, to get a description of the dynamics.

3.1. Effect of heterogeneity

As shown in Fig. 4, the crack pattern becomes more irregular with increasing heterogeneity. This is because with increasing σ^2 the probability that a crack changes its direction, due to local heterogeneities of the threshold ϵ_{ij}^b, increases. Moreover, there is an increasing number of springs with $\epsilon_{ij}^b \ll \bar{\epsilon}$ which break without inducing the formation of a larger crack. This leads to a large number of small isolated cracks.

In Fig. 5 this phenomenology is quantified in terms of the Minkowski densities during crack formation. The formation of cracks starts earlier for higher heterogeneity. However the development of the crack network is more gradual compared to the more homogeneous case. Here, the crack pattern is developed abruptly once the process is initiated, i.e. once the relaxed spring length λ has fallen below a critical value. This characteristic effect of heterogeneity can be seen very clearly from the dynamics of the area and the length density of the cracks. The

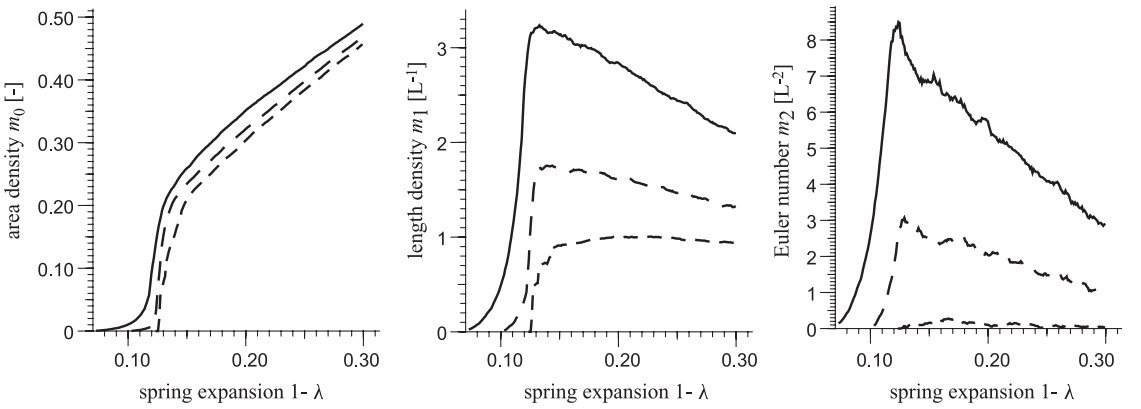

Fig. 5. Dynamics of area density (left), length density (middle) and Euler number (right) of simulated crack patterns with increasing heterogeneity (σ^2=0.1, 0.15, 0.2) shown with increasing dash length.

Euler number as well as the length densities reflect the increasing number of isolated cracks with increasing heterogeneity.

The occurrence of a large number of isolated cracks as obtained for high heterogeneities is not reported in the literature and was also not observed in our own experiments (Vogel et al., 2004). This raises the question if the physical base of our model is false, or if the model ignores other processes that are relevant in nature. Plastic deformation which is ignored in our model should produce even more isolated cracks, since the zone of influence of individual cracks is reduced as discussed below for the parameters of friction and relaxation intensity. On the other hand such microscopic failures may also occur in nature but they might be difficult to detect because they are too small. In our model the spatial resolution is restricted by the separation of nodes which is of the order of 1/10 to 1/100 of the size of aggregates. In clay, the ratio between the size of clay minerals and the size of aggregates is typically much smaller so that individual microscopic defects might not be visible. Though less important for water flow, these microscopic defects are expected to have a significant effect on the strength of the material and thus on the developing crack pattern at lower water content.

3.2. Effect of friction

Qualitatively, Fig. 4 shows that the width of cracks and the size of aggregates decrease with increasing friction. This can be expected since friction restrains the movement of nodes and thus limits the width of individual cracks. As a consequence, the total energy in the center of the aggregates increases so that more cracks are generated here. In summary, the characteristic length scale of the crack pattern becomes smaller and the irregularity of the pattern increases with increasing friction.

The area and length densities (Fig. 6) during crack formation indicate that for larger friction μ the crack pattern is formed later, meaning at a higher level of global energy. However the Euler number shows that the first cracks appear at the same critical energy, which has to be expected since mean and variance of the threshold ϵ^b are the same for the different simulations. With increasing friction, however, the self-accelerated process after the initial crack formation is retarded because the movement of the nodes is restricted by friction. The increasing number of isolated cracks as a consequence of increasing friction is reflected by the Euler number. This is true at the beginning as well as during crack formation where new cracks appear inside aggregates.

The friction parameter could be related to the thickness of the clay layer since the influence of the non-shrinking base, and herewith the friction, decreases with increasing thickness of the layer. The correlation between the size of aggregates and the thickness of the shrinking layer was demonstrated experimentally for various materials from coffee powder (Groisman and Kaplan, 1994) to alumina/water slurry (Shorlin and de Bruyn, 2000).

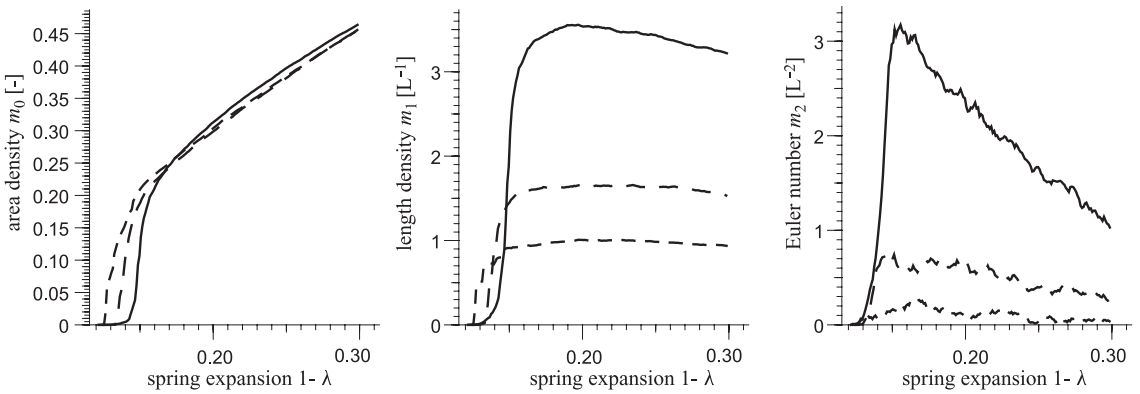

Fig. 6. Dynamics of area density (left), length density (middle) and Euler number (right) of simulated crack patterns with increasing friction (μ=0.0025, 0.005, 0.01) shown with increasing dash length.

3.3. Effect of relaxation intensity

The relaxation parameter n_{it} affects the crack pattern in a similar way as the friction (Fig. 4). The common physical aspect is that the zone of influence of a single broken spring is reduced when the relaxation parameter becomes smaller which is the same for an increased friction. Consequently, more cracks are formed independently leading to a more dispersed crack pattern. However, in contrast to an increased friction the shrinkage process is not stopped but only slowed down by a reduced relaxation intensity, so that the self accelerated process of crack formation is less disturbed compared to the case of high friction. Consequently the resulting crack pattern shows less isolated small cracks in the center of aggregates.

The similarity between the effect of friction and relaxation intensity is reflected by the dynamics of the area density of cracks (Fig. 7). The retarded movement of nodes at low values of n_{it} leads to a retarded development of the crack pattern as with high values of μ. However the dynamics of the length density and the Euler number are different. Once the crack network is formed, indicated by the sharp maximum of m_1, the aggregates shrink gradually without the creation of new isolated cracks and the Euler number decreases due to the coalescence of initially independent cracks.

The relaxation parameter of the model could be related to the intensity of the desiccation process. It is a measure of a characteristic time available for equilibration of local energy gradients between single

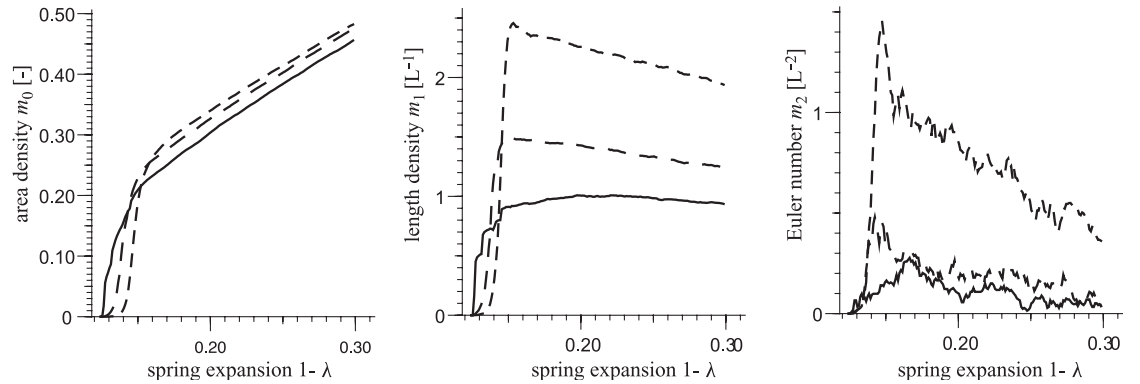

Fig. 7. Dynamics of area density (left), length density (middle) and Euler number (right) of simulated crack patterns with increasing relaxation intensity (n_{it}=4, 9, 15) shown with increasing dash length.

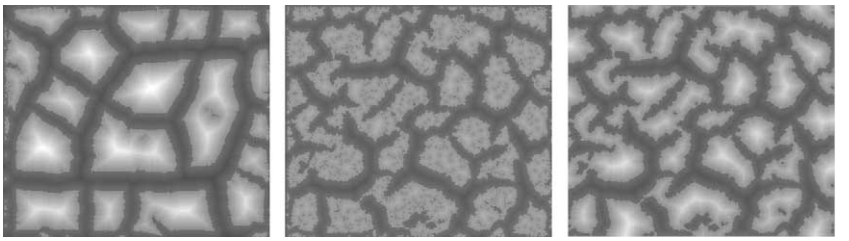

Fig. 8. Distance maps of crack patterns shown in Fig. 4: P1 (left), P2 (middle) and P2 after removing the isolated small cracks (right). The grey level corresponds to the orthogonal distance of each pixel to the boundary of the crack network.

crack events. Naturally, this time becomes shorter with increasing rate of water evaporation.

3.4. Minkowski functions of final crack patterns

Up to now, we analyzed the dynamics of the simulated crack patterns qualitatively and quantitatively by means of Minkowski densities. To compare the final crack patterns in more detail, we calculated the Minkowski functions as proposed by (Vogel et al., 2004). Thereby, the Minkowski numbers—area, length and Euler number—are measured for subsets with a given minimum distance to the crack boundary. This was done for regions within aggregates and within cracks. The different subsets are obtained from 'distance maps' of the structure containing the orthogonal distance of each pixel to the crack boundary as its grey value. The distances are obtained through morphological erosions by various distances r of the cracks and the aggregates, respectively (Vogel et al., 2004). Examples for the distance maps of the crack pattern P1 and P2 (Fig. 4) are shown in Fig. 8. Due to the larger aggregates in P1 we find larger distances, i.e. higher grey levels within the aggregates. The crack pattern P2 contains many small isolated cracks in the center of the aggregates. These small cracks are typically formed by single broken springs, with a scale clearly separated from the length scales of the macroscopic crack network. In the following, our analysis is focused on the macroscopic crack network and we thus removed the small cracks prior to the measurement of Minkowski functions. The distance map of P2 after removing the microcracks is also shown in Fig. 8.

The Minkowski functions of the extreme patterns in Fig. 4, P1–4, are shown in Fig. 9. For $r<0$ we consider subsets within the cracks, for r>0 subsets within the aggregates and for $r=0$ the Minkowski densities of the original crack patterns are recovered.

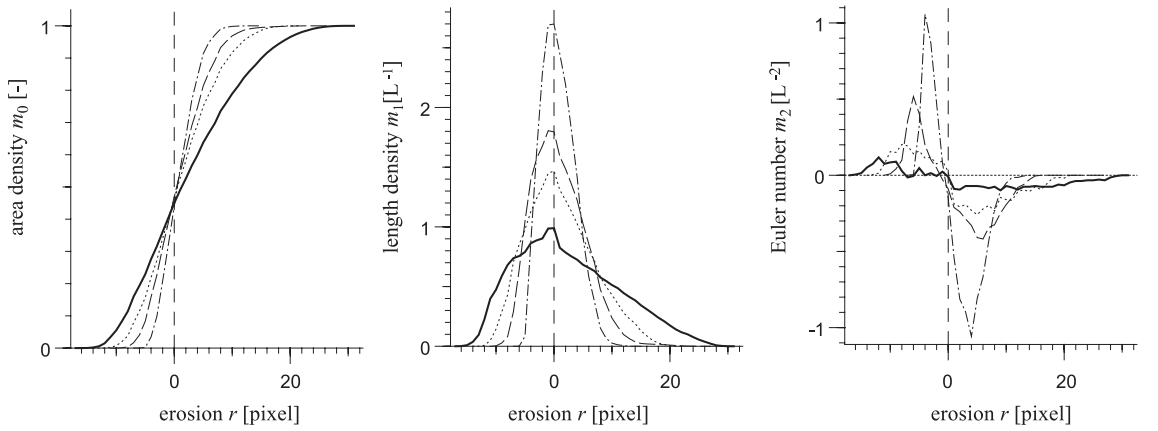

Fig. 9. Minkowski functions of area density (left), length density (middle) and Euler number (right) for the extreme crack patterns shown in Fig. 4: P1 solid line, P2 dotted, P3 dashed, and P4 dashed-dotted. Subsets within the cracks are indicated with negative r, those within aggregates with positive r.

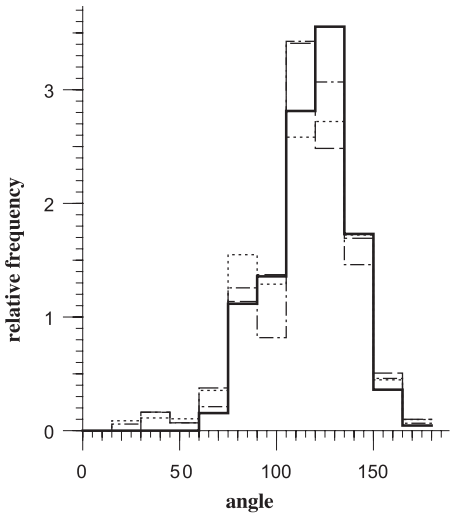

Fig. 10. Frequency distribution of bifurcation angles for the extreme crack patterns shown in Fig. 4: P1 solid line, P2 dotted, P3 dashed, and P4 dashed dotted.

The latter correspond to the results obtained for the maximum of $1-\lambda$ in Figs. 4–6 with the microcracks ignored. The area density function $m_0(r)$ indicates an almost identical total surface area of cracks for all simulations. This can be explained by the threshold $\bar{\epsilon}^b$ and the maximum expansion of springs, $1-\lambda$, which was the same for all simulations. However the different size distribution of cracks and aggregates is clear from $m_0(r)$. The characteristic lengths decrease in the order P1>P2>P3>P4 which corresponds to the effect of heterogeneity>relaxation intensity>friction for the parameter space considered here. The length density functions $m_1(r)$ also reflects the different size distribution. It becomes increasingly peaked in the same order as the characteristic lengths becomes smaller. The Euler number $m_0(r)$ describes the size distribution of cracks and aggregates in terms of their number density. The maximum of $m_0(r)$ for $r<0$ counts the number of cracks and is shifted towards smaller distances with decreasing characteristic length. The same is true for the number density of aggregates evaluated by $r>0$.

The dynamics of the Minkowski numbers (Figs. 4–6) together with the Minkowski functions (Fig. 9) provide a first order geometric description of the simulated crack patterns. The systematic evaluation of the parameter space demonstrates the potential of our model to describe various patterns. The experimental results obtained by Vogel et al. (2004) for homogeneous mixtures of sand and bentonite lay within the prospects of our model.

3.5. Angles of bifurcation

As an additional measure to characterize the form of the crack pattern we determined the distribution of angles within the crack network as described by Vogel et al., 2004. The angles are divided into 12 classes between 0° and 180° and the relative frequency of each class was determined. As shown in Fig. 10 this distribution is similar for all simulations with a clear maximum around 120°. Another maximum was found at around 90°. The latter is more striking for the simulations with increased friction and with increased heterogeneity. Here, more isolated cracks are formed that rejoin existing cracks preferably at an angle of 90°. This typical frequency distribution was also found in experiments (Vogel et al., 2004) for different mixtures of sand and bentonite. It can be seen as direct consequence of the energy distribution within the lattice of springs during crack formation as discussed above. It should be noted that the geometry of the underlying lattice of springs suggests the formation of bifurcations at an angle of 120°. We found that for low heterogeneities, i.e. $\sigma^2 \rightarrow 0°$, the underlying lattice clearly determines the angles of the crack pattern (results not shown). However, with increasing heterogeneity the pattern becomes apparently independent of the lattice geometry.

4. Conclusions

We presented a model of crack formation which aims at mimicking the underlying physical processes. The model is based on a lattice of Hookean springs of finite strength. Shrinkage of a pseudo two-dimensional clay surface is thus idealized by a linear elastic process which is interrupted by the occurrence of cracks. Through a systematic evaluation of the parameter space we demonstrated the potential of the model to describe natural crack patterns including their dynamics. In particular:

- the model reproduces the characteristic dynamics of crack formation in clay as quantified by the

evolution of Minkowski densities during crack formation.
- the model reproduces characteristic features of natural crack patterns as quantified by Minkowski functions and the distribution of bifurcation angles.
- the parameters of the model have immediate physical meaning and hence, can be directly linked to physical material properties and boundary conditions.

This implies promising prospects for the characterization of the dynamics of clay soils or other swell–shrinking materials. The crack pattern at the soil surface which is easily accessible could be analyzed to estimate the model parameters. Then, the dynamics of the crack network as well as the dynamics of the bulk density of the aggregates is provided by the model. This opens the perspective to couple our model to state-of-the-art models of flow and transport in soil including the phenomena of preferential flow along macropores. Such models currently use ad hoc formulations of separated flow domains, i.e. fast macropore flow and slow matrix flow, where the respective volume fractions are obtained by fitting the model to experimental observations. Our crack model has the potential to be extended to three-dimension through either simple assumptions on the penetration depth of cracks or by an explicit representation of the three dimensions together with a full coupling with models for water flow. Then, the crack model could provide the fraction of macropores including their topology and dynamics. Moreover, the dynamics of bulk density may be used for scaling of the hydraulic properties of the matrix domain. So far, our model is a first step towards this direction.

References

Askar, A., Jin, Y., 2000. Macroporous drainage of unsaturated swelling soil. Water Resour. Res. 36, 1189–1197.

Chertkov, V.Y., 2000. Using surface crack spacing to predict crack network geometry in swelling soils. Soil Sci. Soc. Am. J. 64, 1918–1921.

Colina, H., de Arcangelis, L., Roux, S., 1993. Model of surface cracking. Phys. Rev., B 48, 3666–3676.

Gerke, H.H., van Genuchten, M.T., 1993. A dual-porosity model for simulating the preferential movement of water and solutes in structured porous media. Water Resour. Res. 29 (1), 305–319.

Greco, R., 2002. Preferential flow in macroporous swelling soil with internal catchment: model development and application. J. Hydrol. 269, 150–168.

Groisman, A., Kaplan, E., 1994. An experimental study of cracking induced by desiccation. Europhys. Lett. 25, 415.

Hallett, P.D., Newson, T.A., 2001. A simple fracture mechanics approach for assessing ductile crack groth in soil. Soil Sci. Soc. Am. J. 65, 1083–1088.

Hallett, P., Dexter, A., Seville, J., 1995. The application of fracture mechanics to crack propagation in dry soil. Eur. J. Soil Sci. 46, 591–599.

Horgan, G.W., Young, I.M., 2000. An empirical stochastic model for the geometry of two-dimensional crack growth in soil (with discussion). Geoderma 96, 263–276.

Hornig, T., Sokolov, I.M., Blumen, A., 1996. Patterns and scaling in surface fragmentation processes. Phys. Rev., E 54, 4293–4298.

Jarvis, N.J., 1994. The MACRO model (version 3.1.). Technical description and sample simulations, technical report, Department of Soil Science, Swedish University of Agricultural Science.

Kitsunezaki, S., 1999. Fracture patterns induced by desiccation in a thin layer. Phys. Rev., E 60, 6449–6464.

Malthe-Sørenssen, A., Walmann, T., Feder, J., Jossang, T., Meakin, P., Hardy, H.H., 1998. Simulation of extensional clay fractures. Phys. Rev., E 58, 5548–5564.

Meakin, P., 1987. A simple model for elastic fracture in thin films. Thin Solid Films 15, 165–190.

Mecke, K., 2000. Additivity, convexity, and beyond: applications of Minkowski functionals in statistical physics. Lect. Notes Phys. 554, 111–184.

Nichols, J.R., Grismer, M.E., 1997. Measurements of fracture mechanics parameters in silty-clay soil. Soil Sci. 162, 309–322.

Perrier, E., Mullon, C., Rieu, M., de Marsily, G., 1995. Computer construction of fractal soil structures: Simulation of their hydraulic and shrinkage properties. Water Resour. Res. 31, 2927–2943.

Shorlin, K.A., de Bruyn, J.R., 2000. Developement and geometry of isotropic and directional shrinkage-crack patterns. Phys. Rev., E 61, 6950–6957.

van Genuchten, M.T., Wierenga, P.J., 1976. Mass transfer studies in sorbing porous media: I. Analytical solutions. Soil Sci. Soc. Am. J. 40, 473–480.

Vogel, H.-J., Hoffmann, H., Roth, K., 2004. Studies of crack dynamics in clay soil: I. Experimental methods, results and morphological quantification. Geoderma 125, 215–223 (this issue).